Ice Cloud and Humidity Distributions Observed by the A-train

Brian H. Kahn (bhkahn@jifresse.ucla.edu)[1,2], Andrew Gettelman[3], Annmarie Eldering[2] , Calvin K. Liang[1,4], and Karen Rosenlof[5]

[1] Joint Institute for Regional Earth System Science and Engineering, University of California–Los Angeles, Los Angeles, CA, USA [2] Jet Propulsion Laboratory, California Institute of Technology, Pasadena, CA, USA [3] National Center for Atmospheric Research, Boulder, CO, USA

[4] Department of Atmospheric and Oceanic Sciences, University of California–Los Angeles, Los Angeles, CA, USA [5] NOAA Aeronomy Lab, Boulder, CO, USA

ABSTRACT

We quantify the variability of relative humidity (RHI) within and outside of ice clouds using coincident, spatially and temporally continuous observations of temperature, water vapor, and cloud properties from AIRS, CALIPSO, and CloudSat. AIRS shows higher RHI values, as well as increased frequency of super-saturation with respect to ice, to be coincident or nearly coincident with cirrus cloudiness in the upper troposphere. Cloudy and clear RH mean and variance fields show strong seasonal, latitudinal, and height dependences. The modulation of these dependences by dynamical processes is investigated using AIRS temperature variability. We show that the spatial and temporal variability of temperature variance explains a significant portion of the spatial and temporal variability of RHI variance. This work suggests that the inference of ice nucleation mechanisms from cloudy RHI distributions, as suggested by previous studies, must first consider dynamical controls on RHI .

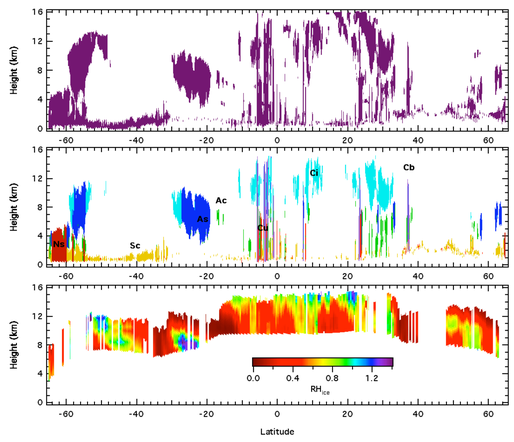

Figure 1. Vertical cross-sections of radar-lidar cloud mask (top), radar-only cloud type (middle), and AIRS-derived RHI (bottom). Shown is an illustrative ascending orbit on 04 June 2007 using CloudSat granule 5852 that coincides with AIRS granules 52–58. Note the relative variation in moist and dry layers that correspond to clouds & clear sky as well as to different cloud types.

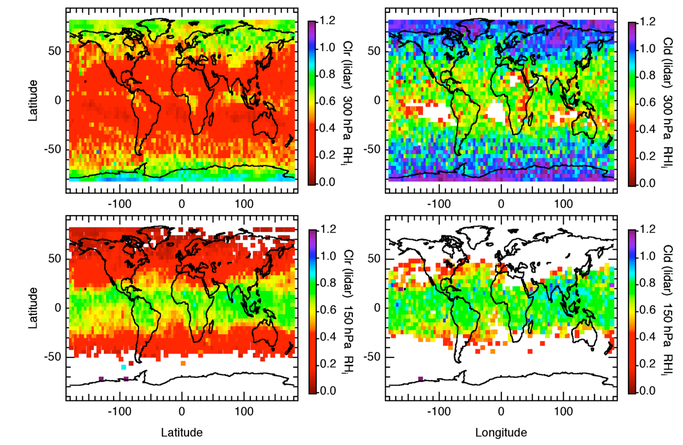

Figure 5. Clear sky (left column) and cloudy sky (right column) RHI defined by the lidar at 300 hPa (top row) and 150 hPa (bottom row) for SON 2006. All AIRS RHI sampling limited to the CloudSat/CALIPSO ground track.

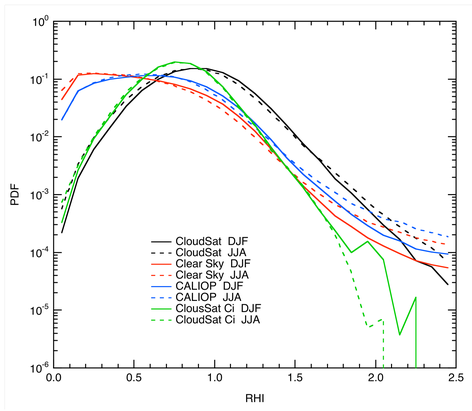

Figure 2. Shown are global 1-D histograms of RHI for DJF in 2006–2007 (solid) and JJA in 2007 (dashed). Clear sky (red) is defined as that observed by the lidar. Cloud is viewed three different ways: by the lidar only (blue), by the radar only (black), and by the radar only for the cloud type "Cirrus" (green) as reported in the R04 2B-CLDCLASS product. Note that RHI is substantially higher within CloudSat-detected clouds compared to CALIOP. This is largely due to the effects of cloud geometrical thickness on the interpretation of RHI.

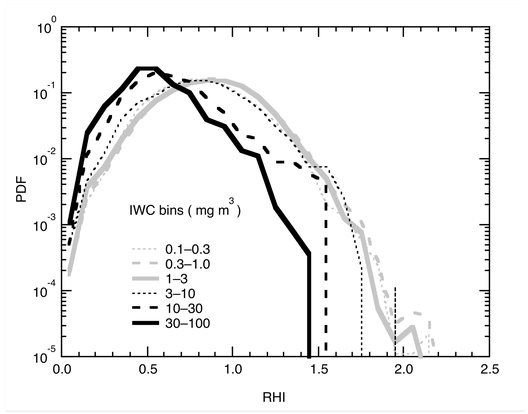

Figure 3. Shown are global 1-D histograms of RHI for five days in late 2006 partitioned by IWC bins (determined by the CloudSat R04 2B-CWC-RO product). Observe that as IWC increases, the RHI distribution shifts towards drier values. This is consistent with the characteristics of cirrus vertical structure and evolution. Also, note the prevalance of supersaturated regions especially for low IWC clouds.

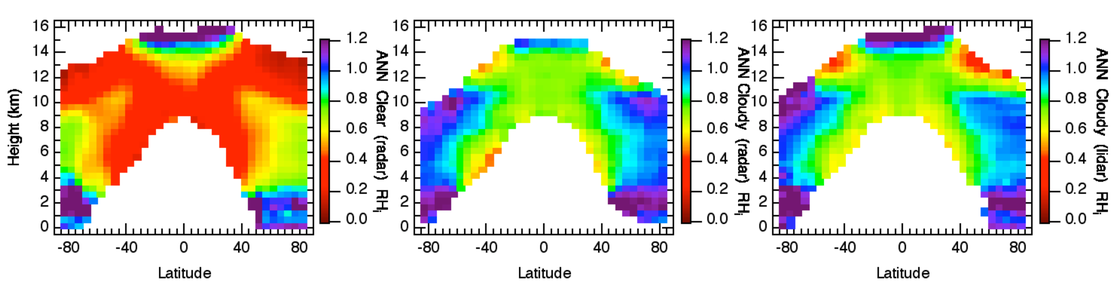

Figure 4. Zonal-averaged cross-sections of the mean RHI in clear sky and within clouds for September 2006 – August 2007. Clear sky (left) is defined by the radar GEOPROF product when the cloud confidence mask = 0. Cloudy sky defined by the radar GEOPROF product (middle) when the cloud confidence mask ≥ 30, and also defined by the clouds detected by the lidar only (right) using the difference of the R04 GEOPROF-LIDAR and GEOPROF products. The RHI from AIRS is limited to "best" and "good" quality control for T(z) and q(z).

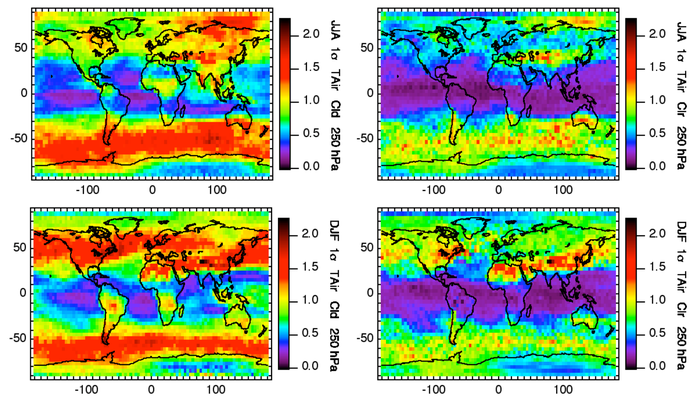

Figure 6. Shown is the seasonal variation of the 1σ T (K) at 250 hPa within cloudy (left) and clear (right) skies. Cloudy AIRS pixels are defined as those with an ECF ≥ 0.05 (averaged over the AMSU FOV). Clouds can be located anywhere in the vertical column, not necessarily at 250 hPa. Note the higher variance in cloudy pixels and in the SH.

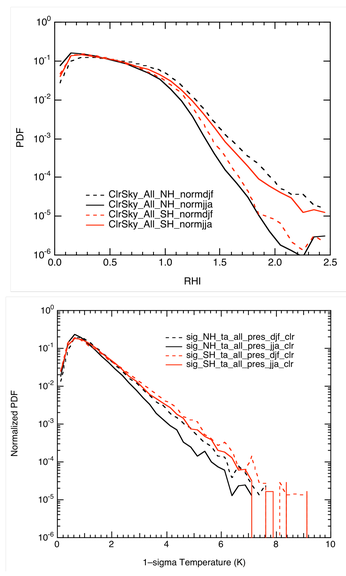

Figure 7. (a) Normalized frequency distributions of RHI for clear sky (top) in the NH (black) and the SH (red) for DJF (dashed) and JJA (solid). (b) Frequency distributions of temperature variability for the same conditions listed in the RHI figure. Note that the strong seasonality in RHI corresponds with temperature variance in the NH, but not in the SH.

Figure 8. Same as Figure 7 except for cloudy sky as defined by the radar. Note that the strong seasonality in RHI again corresponds with temperature variance in the NH. In the SH, there is little seasonality in RHI, which is consistent with the marginal seasonality in temperature variance.

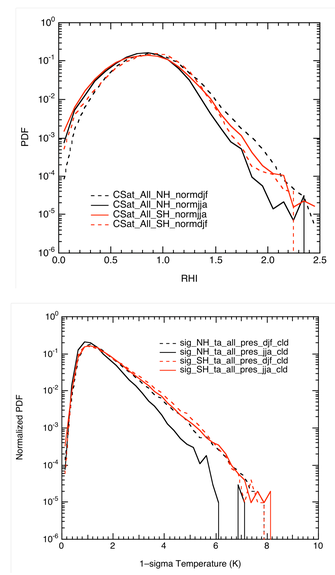

Results

- Collocated temperature, specific humidity, and cloud profiles from AIRS, CloudSat, and CALIPSO reveal new information about humidity fields within and outside of tenuous cloud structures
- Inverse relationship between IWC and RHI suggests importance of microphysical processes
- Climatology of RHI within and outside of tenuous ice clouds will be useful for climate model evaluation
- Histograms of RHI and T variance suggest that inter-hemispheric differences in RHI are possibly caused (to first order) by dynamical differences, not anthropogenic effects, as suggested in some previous studies.

Acknowledgments: A portion of this work was performed at the Jet Propulsion Laboratory, California Institute of Technology.